Bioconjugate Chemistry

Article

pubs.acs.org/bc

Alexa Fluor-Labeled Fluorescent Cellulose Nanocrystals for Bioimaging Solid Cellulose in Spatially Structured Microenvironments

Jay W. Grate,* Kai-For Mo, Yongsoon Shin, Andreas Vasdekis, Marvin G. Warner, Ryan T. Kelly, Galya Orr, Dehong Hu, Karl J. Dehoff, Fred J. Brockman, and Michael J. Wilkins

Pacific Northwest National Laboratory, P.O. Box 999, Richland, Washington 99352, United States

Supporting Information

ABSTRACT: Methods to covalently conjugate Alexa Fluor dyes to cellulose nanocrystals, at limiting amounts that retain the overall structure of the nanocrystals as model cellulose materials, were developed using two approaches. In the first, aldehyde groups are created on the cellulose surfaces by reaction with limiting amounts of sodium periodate, a reaction well-known for oxidizing vicinal diols to create dialdehyde structures. Reductive amination reactions were then applied to bind Alexa Fluor dyes with terminal amino-groups on the linker section. In the absence of the reductive step, dye washes out of the nanocrystal suspension, whereas with the reductive step, a colored product is obtained with the characteristic spectral bands of the conjugated dye. In the second approach, Alexa Fluor dyes were modified to contain chloro-substituted triazine ring at the end of the linker section. These modified dyes then were reacted with cellulose nanocrystals in acetonitrile at elevated temperature, again isolating material with the characteristic spectral bands of the Alexa Fluor dye. Reactions with Alexa Fluor 546 are given as detailed examples, labeling on the order of 1% of the total glucopyranose rings of the cellulose nanocrystals at dye loadings of ca. 5 μg/mg cellulose. Fluorescent cellulose nanocrystals were deposited in pore network microfluidic structures (PDMS) and proof-of-principle bioimaging experiments showed that the spatial localization of the solid cellulose deposits could be determined, and their disappearance under the action of Celluclast enzymes or microbes could be observed over time. In addition, single molecule fluorescence microscopy was demonstrated as a method to follow the disappearance of solid cellulose deposits over time, following the decrease in the number of single blinking dye molecules with time instead of fluorescent intensity.

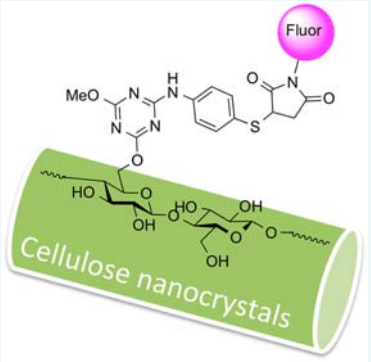

INTRODUCTION

Cellulose is an abundant natural solid carbohydrate biopolymer. There is increasing interest in methods to conjugate dyes, polymers, biomolecules, and other moieties onto cellulose and cellulose-derived nanostructures (including fibers, particles and nanocrystals) for bioimaging, material science, sensors, and other technological applications.[1−8] Cellulosic materials and nanocrystals are also of interest in drug delivery, gene transfection, and other biomedical applications.[9−13] Motivation for the use of polysaccharide nanoparticles for targeted drug delivery, and for fluorescent cellulose nanostructures in particular, have been set out by Dong and Roman.[2] Here we are interested primarily in the global significance of cellulose as a carbon pool that is subject to environmental and microbial processes. Cellulose is of profound importance in the biosphere as carbon cycles between atmospheric carbon dioxide, plant cellulose, and terrestrial soil environments, and hence plays a significant role in the global carbon budget.[14−16] It has been proposed that a relatively small change in the balance between how carbon is stored or cycled in terrestrial environments could mitigate anthropogenic carbon dioxide emissions if carbon storage is increased, or intensify climate change if carbon storage in soil is decreased.[17] Accordingly, the study of processes involving cellulose is of significant research interest. Cellulose, however, is not soluble in aqueous environments. Moreover, solid cellulose degradation in terrestrial ecosystems does not occur in either homogeneous or heterogeneous batch reactors; it occurs in spatially structured heterogeneous microenvironments such as soils and sediments. Hence, two technical challenges arise: (1) solid cellulose processing and deposition into microstructured model environments, and (2) bioimaging solid cellulose location and degradation in such model environments.

Conventional methods for assaying enzymatic degradation of cellulose, using isolated enzymes or living microorganisms, entail batch reactions where the sugars released into solution are assayed after separating the solid cellulose from the batch aqueous suspension.[18] The reducing sugars released by hydrolysis of undyed cellulose solids are determined from aldehyde assays, while measurements starting with dyed

Received: January 21, 2015
Revised: February 20, 2015
Published: March 2, 2015

DOI: 10.1021/acs.bioconjchem.5b00048
Bioconjugate Chem. 2015, 26, 593−601

cellulose determine the absorbance due to the released dyed sugars. Cellulose materials dyed with fluorescent 5-(4,6-dichlorotriazinyl)aminofluorescein (DTAF) have been assayed similarly, centrifuging undissolved cellulose solids down before measuring released fluorescent cellodextrins.[19]

It would be advantageous to develop methods to study cellulolytic processes in observable spatially structured microenvironments, and imaging the *local losses of solid cellulose* rather than the batch generation of sugars. Such observations in natural settings with opaque soil and sediments are difficult, but could be carried out in laboratory studies in spatially structured microfluidic devices. Such studies would require the following two characteristics: (1) a form of cellulose that can be deposited in spatially structured environments, which is normally a challenge due to the fibrous insoluble nature of solid cellulose, and (2) fluorescent tagging so that modern microscopy methods can be used to follow cellulolytic processes, using modern dyes with good photostability.

Here we solve the first problem by using cellulose nanocrystals[20−26] as a form of cellulose that can be suspended in solvents and applied into films or localized solids at the microscale. Digestion of amorphous cellulose domains from native cellulose releases the more slowly digestible microcrystalline domains of microfibrils as cellulose nanocrystals (cnxtls).[22,23,25] Although microcrystalline cellulose from natural sources autofluoresces, our measurements have shown that the intrinsic fluorescence of unlabeled cnxtls is initially low and rapidly photobleached. We are interested in cnxtls that are coupled to modern fluorescent dyes.

Cellulose nxtls have been dyed previously with fluorescein-5′-isothiocyanate (FITC) after modifying the cnxtl surfaces with epichlorohydrin to create an epoxide that was opened with ammonia, providing an amine for dye linkage.[2] Cellulose nxtls have been doubly labeled with dyes for pH sensing by reacting native surface hydroxyls directly with FITC and Rhodamine B isothiocyanate (RBITC) dyes in basic solution to form thiocarbamate linking bonds.[8] Cellulose nxtls have also been derivatized with coumarin dyes, ethynylferrocene, or imidazolium using click chemistry, after modifying the cnxtls hydroxyl groups creating azide or alkynyl substituents.[3,5,27] Suspended starch particles have been modified with Alexa Fluor 488 azide after an enzyme catalyzed esterification with 10-undecynoic acid.[28]

We are particularly interested in cnxtls-labeled with modern Alexa Fluor dyes for imaging applications.[29] These dyes have superior brightness and photostability, and some can be used in single molecule fluorescence microscopy techniques. In the present study we have investigated the covalent dying of cnxtls with Alexa Fluor dyes using chemical approaches that will react with unmodified cellulose surfaces or with oxidized dialdehyde cellulose surfaces. We have shown that these fluorescent cnxtls can be deposited as local resource islands in pore network microfluidic devices, and shown using fluorescent microscopy that localized solid cellulose deposits hydrolysis can be observed.

RESULTS AND DISCUSSION

Cellulose Nanocrystals. In the present study, cnxtls prepared with a well-known sulfuric acid digestion method,[20] or a more recently developed hydrobromic (HBr) acid digestion method,[5,7,21] served as the starting point for developing fluorescently dyed cellulose material suitable for deposition in spatially structured microfluidic devices. We prefer cnxtls prepared using HBr because, unlike sulfuric acid, it does not functionalize the surfaces with sulfate half esters. Although this provides a more natural cellulose material, the HBr-digested nanocrystals are somewhat more prone to aggregation. AFM images of undyed and dyed cnxtls confirm the nanostructured nature of the material (Supporting Information Figure S1).

Labeling reactions have been performed on unmodified cnxtls using triazine reagents that react directly with hydroxyl groups, and on cnxtls that have first been oxidized to create dialdehyde structures suitable for reactive labeling. The latter approach will be described first. In all labeling work, our objective has been to convert only small percentages or less of the glucopyranose units to fluorescent derivatives, so that the material will predominantly appear as natural cellulose, while still having sufficient dye so that solid deposits can be observed and followed using fluorescence microscopy. While the individual nanocrystals are dyed only on the surfaces, aggregates and deposits consisting of many nanocrystals will have dye labels throughout the solid deposited material.

Dye Modifications. Maleimide terminated Alexa Fluor dyes were modified by reactions as shown in Scheme 1, using

Scheme 1. Modification of Alexa Fluor 546 C_5 Maleimide.[a]

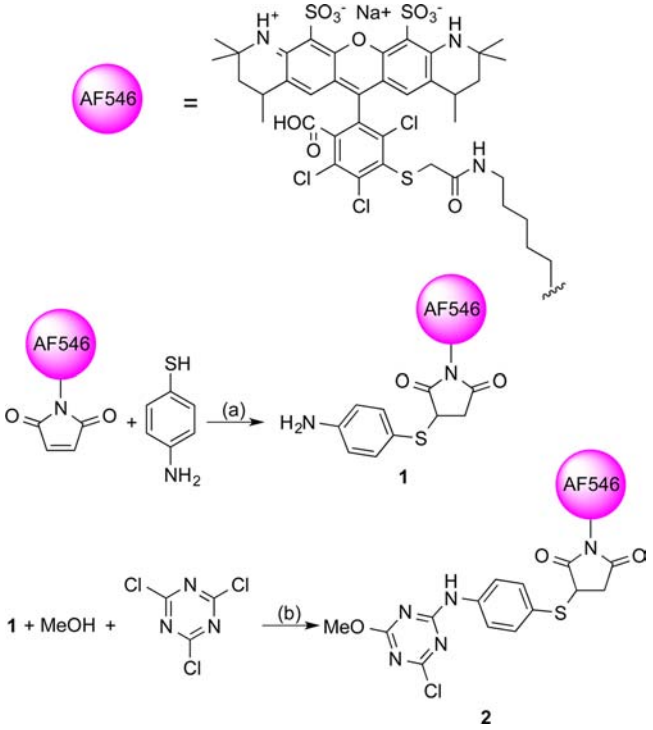

[a]Reagents and conditions: (a) MeOH; (b) Na_2CO_3, MeOH/CH_3CN, 0 °C.

Alexa Fluor 546 C5 maleimide as the exemplary case. In general, our studies have used Alexa Fluors 546 and 647. For reductive amination reactions on dialdehyde-modified cnxlts (DA-cnxtls), the maleimide was reacted with 4-aminothiophenol in methanol to generate **1** as the labeling reagent. Further reaction of **1** with cyanuric chloride provided a reagent for direct labeling of cellulose hydroxyl groups. Triazine chemistry using cyanuric chloride will be described in more detail below with reference to reactions on unmodified cnxtls. Each dye modification method is described in the Experimental

DOI: 10.1021/acs.bioconjchem.5b00048
Bioconjugate Chem. 2015, 26, 593−601

Procedures with their respective cellulose labeling reactions. Both compounds **1** and **2** were confirmed by HR-ESI-QTof MS (Supporting Information Figures S2−S5).

Conjugation to Oxidized Cellulose Nanocrystal Surfaces. The reaction of cellulose with periodate to convert adjacent hydroxyl groups to paired aldehyde groups is a well-known chemistry[30−32] whose specificity has historically been used in the structural analysis[33,34] of carbohydrates. Although the bond between glucopyranose ring carbons in positions 2 and 3 is broken in this reaction, the linear polymer chains are not cleaved to shorter units under typical conditions. Our goal, to partially oxidize cellulose at the surface to create reactive aldehydes for labeling reactions, differs from studies seeking to completely convert solid cellulose to dialdehyde cellulose material, where crystallinity can be a barrier to full conversion.[30−32] High degrees of oxidation are known to lead to amorphous cellulose-derived product (e.g., 80% conversion).[30] Recently, the reaction of periodate with Cladophora-derived cellulose, using a 5-fold excess of periodate and 10 days reaction time, was described as a convenient one pot method to convert fibrous cellulose to beads of dialdehyde cellulose at 80−100% conversion.[32]

We confirmed the action of limiting periodate quantities on solid cellulose using Avicel PH 301-NF microcrystalline cellulose. Sodium periodate was added to aqueous suspensions of Avicel in amounts that could quantitatively convert 1.2%, 1.5%, or 5.0% of the glucopyranose units to dialdehyde units. The recovered solid products were dispersed in excess known hydroxylamine hydrochloride and the released HCl was back-titrated with NaOH to determine the dialdehyde content. These results indicated 1.17%, 1.47%, and 4.85% conversion to dialdehyde, respectively, and hence 97−98% conversion relative to the limiting periodate reagent. The appearance of a carbonyl band at 1720 cm^{-1}, which was not observed in the initial Avicel, was observed in the oxidized products, while XRD[30] showed that the products remained detectably crystalline, with consistent peak ratios among the modified and unmodified materials. These results confirmed that the periodate reaction under periodate-limited conditions produced predictable conversions, while leaving the bulk material properties (e.g., crystallinity) intact. Higher degrees of oxidation are known to lead to amorphous cellulose-derived product (e.g., 80% conversion).[30] Recently, the reaction of periodate with Cladophora-derived nanocellulose was described as a convenient method to prepare beads of dialdehyde cellulose.[32]

Cellulose nxtls in aqueous suspension were similarly oxidized with sodium periodate with a target of 1% conversion of glucopyranose units, as described in the Experimental Procedures. Typically, a solution of never dried cellulose nanocrystals was reacted with $NaIO_4$ in dark for 3 days and the resulting modified cnxtls were collected by centrifugation, washed with deionized H_2O, and resuspended in deionized H_2O to give a 5 mg/mL solution. The absorption band at 1720 cm^{-1}, corresponding to the C═O stretching of the aldehyde groups, was again observed (Supporting Information Figure S6). and titrations indicated at least 80% conversions. We call these DA-modified cnxtls (DA = dialdehyde).

Reductive amination was used to label these DA-modified cnxtls according to Scheme 2, generating material **3**; details are provided in the Experimental Procedures. Dyed cnxtls in suspension displayed the characteristic absorbance and fluorescence spectra of the Alexa dye, complicated by scattering from the cellulose nanocrystals (Supporting Information

Scheme 2. Synthesis of Dyed Cellulose Nanocrystals by Reductive Amination.[a]

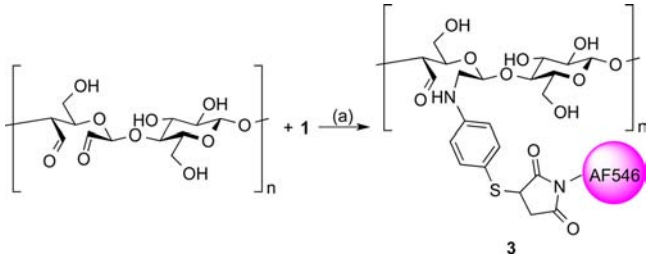

[a]Reagents and conditions: (a) MeOH, AcOH, 40 °C, then 1 M $NaCNBH_3$/THF, 40 °C.

Figures S7 and S8). Using an amount of dye that is stoichiometric with the available aldehyde groups, the recovered product is visibly colored. The absorbance band was compared with a calibration curve generated from known solutions of the free dye to determine that the amount of dye grafted to the cellulose nanocrystals was 6.3 μg/mg cellulose. This amount represents ca. 10% of the original dye in the reaction bound to the DA-modified cnxtls, and 0.1% of the total glucose units modified. Approximately 12% of the oxidized glucose units (6% of the aldehyde groups) were modified.

It was noteworthy in this reductive amination approach that if the reduction step was not carried out, the dye washed out of the material to yield colorless cnxtls. We take this as evidence for covalent bonding between the dye and the cnxtls when the full reductive amination procedure is used to "fix" the bonding with irreversible single bonds. We also take these results as evidence that unbonded dye does not irreversibly adsorb to nanocrystal surfaces, yielding colored material by noncovalent binding processes.

Conjugation on Unaltered Cellulose Nanocrystal Surfaces. For unmodified cnxtl surfaces, we have adapted chemistry using cyanuric chloride to modify the Alexa Fluor dyes to react covalently with hydroxyl groups on the cellulose nanocrystal surfaces. The cyanuric chloride reagent[35] was used to develop reactive dyes for colorfast cotton fabrics[36,37] (cotton being cellulose), and has recently been demonstrated as an elegant chemistry for attaching intact saccharides to array chips.[38] An advantageous feature of cyanuric chloride is that with each nucleophilic substitution of a reactive chloro-group on the triazine ring, the remaining groups become notably less reactive. Typically, nucleophilic attack replaces the first chlorine atom at ice temperatures, while reaction of the next chlorine atom occurs at or above room temperature. The last chloride is not reactive until elevated temperatures are employed.

Under the reaction conditions in Scheme 1 and the Experimental Procedures, we prepared compound **2**, where cyanuric chloride is substituted with one dye molecule covalently attached and one methoxy group. Surprisingly, one of the chloro groups in cyanuric chloride was replaced by a methoxy group even though the reaction was carried out at 0 °C. This structure was confirmed by mass spectrometry, finding m/z of 1301.1223 vs m/z of 1301.1339 calcd for **2** ($C_{53}H_{53}Cl_4N_8NaO_{13}S_4$ $[M + H]^+$) by high resolution ESI-QTof MS.

To conjugate the modified dye **2** to cellulose, temperatures of 60 °C or higher were used to obtain the reaction on the last chloride atom of the triazine ring, as shown in Scheme 3. A cnxtls suspension in dry acetonitrile was mixed with modified

DOI: 10.1021/acs.bioconjchem.5b00048
Bioconjugate Chem. 2015, 26, 593−601

Scheme 3. Synthesis of Dyed Cellulose Nanocrystals Using Triazine Chemistry[a]

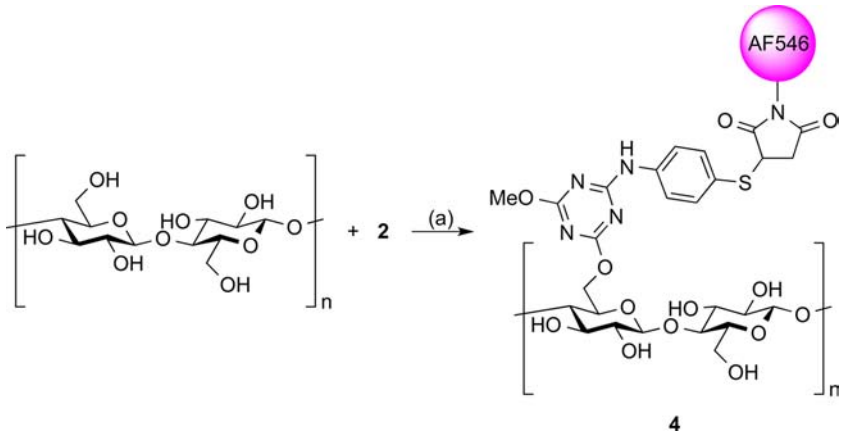

[a]Reagents and conditions: (a) Na_2CO_3, CH_3CN, 65 °C.

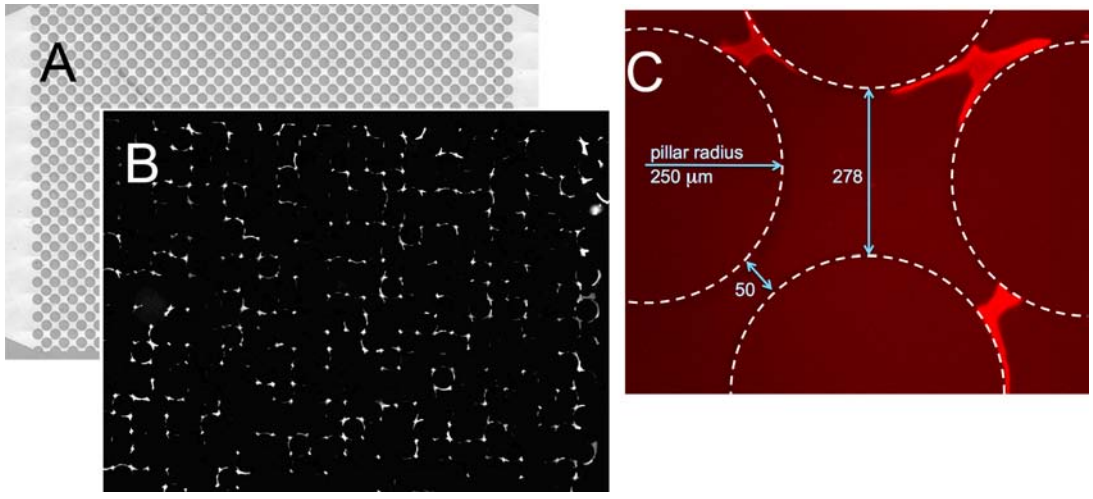

Figure 1. A. Pore network microfluidic structure fabricated in PDMS by a micromolding technique, showing the pillars (gray) and edges (gray), defining the flow paths and pore network (lighter gray). Pillars are 500 μm in diameter and channels are 90 μm deep. The pore throats are 50 μm across, the distance between pillars through the center of a pore is 278 μm, and the pore network area is 15 by 21 mm. Single inlets and outlets are at each end in triangular input areas (not shown). B. Alexa Fluor 647-dyed (from the commercially available Alexa Fluor 647 C2 maleimide and triazine chemistry) cnxtls deposited in a PDMS pore network micromodel, showing one-quarter of the pore network area, where cnxtl deposits appear white in the fluorescent image. C. Pseudocolored image zoomed in on a single pore defined by four pillars, showing the distribution of cnxtls (red) in the pore throats. Pillar locations are delineated with the dashed circles. For B and C, fluorescent images were acquired with a Nikon Eclipse-2000TE epifluorescence microscope equipped with a monochrome CCD camera and a motorized stage, using the Cy5 filter cube.

Alexa Fluor 546 (**2**) and sodium carbonate and the resulting solution was heated to 65 °C in the dark for 36 h to give **4**. The dye-labeled cnxtls were then washed multiple times with MeOH, DMF, DMSO, and water successively to remove any unconjugated dye. Details are provided in the Experimental Procedures. These dyed cnxtls displayed the characteristic absorbance and fluorescence spectra of the Alexa dye (Supporting Information Figures S9 and S10). From the absorbance band it was determined that the amount of dye grafted to the cnxtls was 3.3 μg/mg cellulose. This amount represents ca. 8% of the original dye in the reaction bound to the cnxtls, and 0.05% of the total glucose units modified. In this reaction the only modification to the cellulose is the conjugation of the dye, in contrast to the approach with DA-modified cnxtls.

This labeling reaction has also been investigated in various other solvents including MeOH, DMF, and DMSO in which compound **2** was soluble. However, the reactions were unsuccessful in all these solvents and the resulting cnxtls remained uncolored. Acetonitrile is the preferred solvent.

Deposition in Spatially Structured Microenvironments. Dyed cnxtls were deposited in microfluidic structures consisting of a homogeneous or heterogeneous pore networks in polydimethylsiloxane (PDMS). Overall structures are shown in the Supporting Information Figure S11, while a homogeneous pore network structure and fluorescent cellulose deposits are shown in Figure 1. Pore network devices such as these, sealed with a transparent glass cover plate for imaging, are called "micromodels".[39−46] An array of cylindrical pillars within the flow channel creates the pore network. A 2 mg/mL suspension of the dyed cnxtls in ethanol was first sonicated, then syringe-injected by hand into the assembled microfluidic device. After filling the micromodel with suspension, the ethanol was allowed to permeate through the PDMS and evaporate. The films were dried and fixed to the surface by baking at 50 °C overnight. In this approach, aggregates of many

DOI: 10.1021/acs.bioconjchem.5b00048
Bioconjugate Chem. 2015, 26, 593−601

cnxtls accumulate primarily within the pore throats between pillars and around the periphery of the pillars, as shown in the epifluorescence microscopy images in Figure 1. These images demonstrate that the dyed cnxtls can be deposited in spatially structured microenvironments and imaged.

Bioimaging Cellulose Deposits in Pore Network Micromodels. Alexa Fluor labeled cnxtls were deposited and imaged in a PDMS micromodel for experiments with enzymes and microbes. Dilutions of the Celluclast enzyme mixture were used for enzymatic hydrolysis. First, after fixing the cnxtls in the pore network micromodel by drying at 50 °C, DI water was introduced at 0.2 uL/min, and then the flow rate was reduced to 0.05 uL/min. Specific locations within the micromodel were selected for monitoring. A composite image of one such location taken immediately after filling is shown in Figure 2.

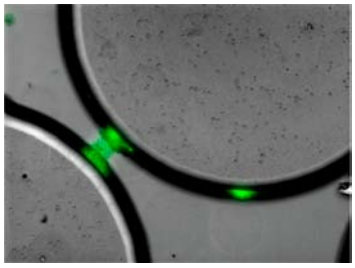

Figure 2. Composite image (gray: bright-field, green: fluorescent cellulose) illustrating a selected portion in the pore network of the micromodel and the spatial localization of the immobilized fluorescent cnxtls (Alexa Fluor 546, triazine labeling method). The image was taken immediately subsequent to water introduction into the micromodel.

Here the green regions are the labeled cnxtl solids while the gray scale shows the pore network structure, where the large circles are pillars and the flow channels are between them. The cnxtls are in the pore throat or on the pillar walls.

Monitoring for 14 h after filling showed no swelling or loss of the solid fluorescent cellulose over time. Then the water was displaced with a 10× dilution of a commercial Celluclast enzyme mixture that hydrolyzes cellulose. Images were recorded at 0, 3, and 7 h, again at a flow rate of to 0.05 μL/min. The fluorescence was largely gone at 3 h(see Supporting Information Figure S12). We interpret the loss of fluorescence as hydrolysis of the cellulose nanocrystals with diffusion and advection of to soluble dye-labeled hydrolysis products (cellodextrins, cellobiose, or glucose) away from the position of the original solid deposit. The solid deposits consist of many nanocrystals aggregated to dimensions of microns, so fluorescent dye labels present on the surfaces of the nanocrystals are distributed throughout the overall deposit. These results show that spatially localized solid cellulose can be imaged in a model heterogeneous microenvironments and its biocatalytic hydrolysis can be qualitatively observed. This provides a model for solid cellulose resource islands in a spatially heterogeneous microenvironment. In additional experiments, with larger deposits and more frequent images, it appeared that the cellulose islands first swell under the action of the Celluclast and then disappear (see Supporting Information Figure S13).

We have also prepared cnxtls-containing pore network micromodels that were inoculated with *Flavobacterium johnsoniae*, a bacterial species that is able to utilize cellulose as its sole carbon source. In addition, the *Flavobacterium johnsoniae* strain had been engineered to constitutively express an mOrange fluorescent protein, enabling visualization of biomass via fluorescence microscopy. A fluorescent image is shown in Figure 3, where the mOrange containing bacteria are

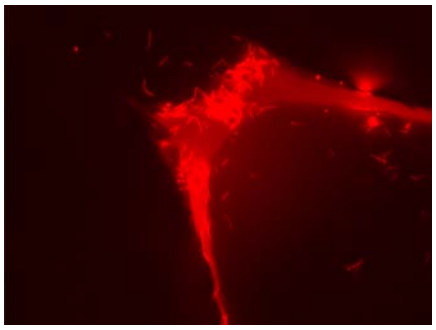

Figure 3. Fluorescent image showing mOrange-expressing Flavobacterium on fluorescent cellulose (Alexa 647, triazine method) in the pore throat of a pore network micromodel.

bright rod shapes of appropriate size, and due to overlap in the spectra of Alexa 647 and mOrange, the fluorescent cellulose deposit is also seen in the image, as a dimmer area in the characteristic shape in a pore throat. This image illustrates the bacterial colonization of the solid cellulose deposit that was present in excess as the carbon source. In repeated cycles of flushing out the pore spaces with additional (carbon free) medium, the bacterial populations within pore spaces were seen to rebound each time, supporting our hypothesis that these strains would be able to grow using the cnxtls. A composite fluorescent image, showing fluorescent cellulose deposits as red and the bacteria as green, (Supporting Information Figure S14) shows the bacterial populations both on the cellulose and free in a pore space. We have also inoculated pore networks with *Cytophaga hutchinsonii*, another species capable of cellulose degradation, and followed the disappearance of spatially localized fluorescent cellulose with time (Supporting Information Figure S15).

Bioimaging Using Single Molecule Fluorescence Microscopy. Using Alexa Fluor 546, a dye with a blinking characteristic, fluorescence could be observed and measured using single molecule fluorescence microscopy, where a low degree of labeling is desirable. Figure 4 illustrates the observation of a portion of a drop-cast film of dyed cnxtls. The cast film was baked at 50 °C for 1 h to dry and fix the cnxtls to the surface. Red ovals in the images highlight specific dye molecules that are blinking, shown "on" in one image and "off" in the other, and therefore indicating that the detected fluorescence spots are indeed single molecules.

After immersing the dried film in a dilute solution of Celluclast (a mixture of cellulase enzymes), an area of cnxtls was monitored continuously and the number of single molecules in this area was counted over time (Figure 5). Hydrolytic release of soluble oligosaccharides and sugars from the solid cellulose, some of which are labeled, reduces the number of dye molecules in the solid film. The released soluble molecules diffuse rapidly in solution. They do not produce diffraction-limited size spots in the fluorescence images, so they are not counted as single molecules. A control experiment without the enzyme showed little decrease in fluorescent dye molecules in the film. Thus, these cnxtls enable observations of cellulose hydrolysis from solid cellulose films using fluorescence

DOI: 10.1021/acs.bioconjchem.5b00048
Bioconjugate Chem. 2015, 26, 593−601

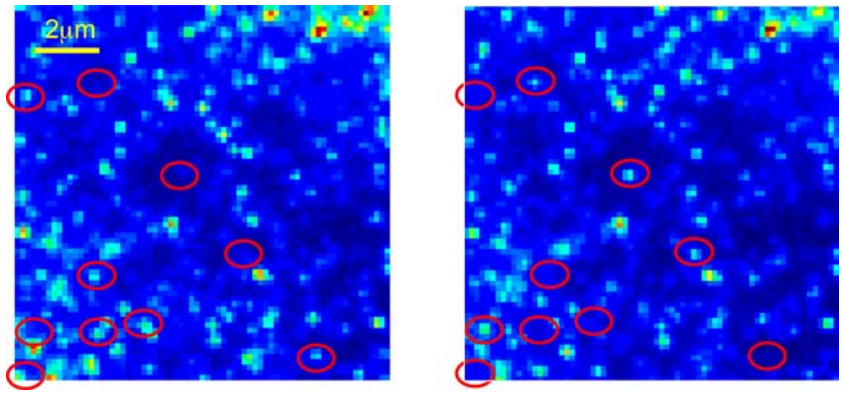

Figure 4. Single molecule fluorescence microscopy of air-dried Alexa Fluor 546 dyed cnxtls on a clean glass surface. The fluorescence from single dye molecules, excited by laser at 532 nm, was recorded by an electron-multiplying CCD camera on an inverted single-molecule fluorescence microscope. The left and right are two consecutive fluorescence images with 0.1 s exposure each. Each pixel is approximately 160 nm on a side, with individual dye molecules shown in spots of 2 × 2 or 3 × 3 pixels. Red ovals highlight specific dye molecules observed to blink on and off in these images. The cnxtls for this sample were prepared by the sulfuric acid hydrolysis method prior to dying.

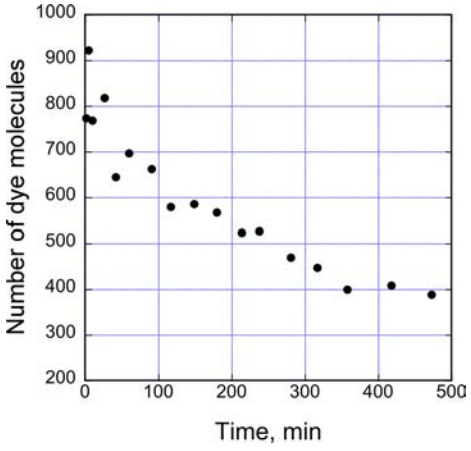

Figure 5. Hydrolysis of Alexa Fluor 546 dyed cnxtls by Celluclast diluted to 4 U/mL in 0.2 mL of 0.1 M pH 5 acetate buffer, measuring the change in the number of single dye molecules in the image field over time for several hours.

microscopy. The single molecule fluorescence microscopy enables changes in fluorescence to be measured as the change in the number of single molecules per area per time, as opposed to the more conventional measure of intensity per area per time.

■ CONCLUSIONS

Two approaches, each with their own potential advantages and disadvantages, have been developed for conjugating modern Alexa Fluor dyes to solid cellulose material for bioimaging applications, using cellulose nanocrystals as a solid cellulose starting material that can be processed into solid deposits in microfluidic structures. Alexa Fluor 546 has been demonstrated as the exemplary dye; however, there are many Alexa Fluor dyes that could be conjugated by this approach, as well as other dyes that can be obtained or converted to amino or maleimide derivatives. For example, we have also conjugated Alexa Fluor 647 starting from the commercially available Alexa Fluor 647 C2 maleimide. Thus, materials can be generated with spectral bands appropriate to the research or application desired, or to provide bioimaging of cellulose with fluorophores whose spectra do not interfere with other fluorophores in the system.

Our intent is to limit the amount of dye conjugated to the cnxtls in order to create materials most closely related to natural crystalline cellulose. The crystalline cellulose is more resistant to degradation than amorphous regions, and hence of particular interest. The triazine chemistry does not alter the material except for the dye attached via native hydroxyl groups. The reductive amination approach both creates oxidized residues and attaches dyes to a fraction of the generated aldehydes. The triazine chemistry requires two reactions to modify the dye, and one reaction to modify the cnxtls; the reductive amination reaction requires only one reaction to modify the dye, but two reactions on the cnxtls.

Several proof of principle bioimaging experiments have shown that these materials can be used to observe and follow the disappearance of spatially localized deposits of solid cellulose materials under the action of hydrolytic enzymes or microorganisms. This approach is in contrast to conventional approaches that follow the hydrolysis of cellulose by analyzing the released sugars after a solid−liquid separation. Furthermore, we have provided a demonstration experiment showing novel single molecule fluorescence microscopy as a means to follow the disappearance of solid cellulose deposits. In addition to enabling observations in spatially heterogeneous microenvironments, as shown above, we anticipate that these materials will also be useful in studying how members of mixed microbial communities associate with solid cellulose deposits.

■ EXPERIMENTAL PROCEDURES

General Information. Reagents were obtained from commercial sources and used as received. Organic solvents were purchased anhydrous and used without further purification. Preparative thin-layer chromatography (TLC) was carried out on Silica Gel F coated on polyester foil (Analtech Inc.) with detection by UV absorption (254 nm) were applicable. Mass spectra were recorded on an Agilent Technologies 6530 Accurate-Mass Q-Tof LC/MS. The calibrant is Standard ESI-L low concentration Tuning Mix with addition of 0.1 mM HP-0321. Fourier transform infrared spectroscopy (FTIR) was measured on a Thermo Scientific Nicolet 6700. UV−visible and fluorescence emission spectra were recorded on a Tecan Safire microplate reader.

Synthesis of Cellulose Nanocrystals. Cellulose nanocrystals were prepared according to the literature proce-

DOI: 10.1021/acs.bioconjchem.5b00048
Bioconjugate Chem. 2015, 26, 593−601

dure.[5,7,21] In general, Whatman no 1 filter paper (2.0 g, 12.3 mmol) in deionized H_2O (200 mL) was blended into pulp by a blender. Water was filtered off and the remaining paper residue was added into 2.5 M hydrobromic acid (100 mL). The resulting reaction mixture was refluxed for 3 h. The hydrolyzed cellulose solution was cooled (0 °C) and ultrasonication (ultrasonic homogenizer) was applied to it for 10 min. The resulting cellulose nanocrytals were collected by centrifugation (5000 rpm, 30 min), washed with deionized H_2O (5 × 50 mL) and resuspended in deionized H_2O (75 mL) to give a 20 mg/mL solution.

Limited Oxidation of Cellulose Nanocrystal Surfaces with Sodium Periodate. To a stirred solution of never dried cellulose nanocrystals (100 mg in 5 mL H_2O, 0.617 mmol) was added $NaIO_4$ (1.32 mg, 6.17 μmol, 0.01 equiv). After stirring for 72 h in the dark, the resulting DA-modified cnxtls were collected by centrifugation (14 000 rpm, 10 min), washed with deionized H_2O (3 × 20 mL), and resuspended in deionized H_2O (20 mL) to give a 5 mg/mL solution. Formation of aldehyde functional groups was confirmed by FTIR measurement with the absorption band at 1720 cm^{-1} corresponding to the C═O stretching (Supporting Information Figure S6). The aldehyde content of DA-modified cnxtls was determined by their reaction with 0.1 M $H_2NOH{\cdot}HCl$ for 24 h followed by titration of the released HCl with 0.1 N NaOH.[30−32] The conversion yields were at least 80%.

Conjugation of Alexa Fluor 546 to Cellulose Nanocrystals by Reductive Amination. To a solution of Alexa Fluor 546 C_5 maleimide (70 μg in 70 μL MeOH, 0.0677 μmol) was added 4-aminothiophenol (18 μg in 18 μL MeOH, 0.14 μmol). The reaction mixture was heated to 35 °C and agitated by the thermomixer in the dark for 2 h (Scheme 1). Another portion of aminothiophenol (18 μg in 18 μL in MeOH, 0.14 μmol) was added and the reaction mixture was kept at 35 °C and agitated in the dark for another 16 h. The reaction progress was analyzed by ESI-QTof MS. Unreacted aminothiophenol was removed by preparative TLC (EtOAc/hexanes, 1/1, v/v) and after evaporation of solvent by a stream of N_2, to give **1** (72 μg, 92%) as a purple solid. High resolution ESI-QTof MS of **1**: *m/z* calcd for $C_{49}H_{51}Cl_3N_5NaO_{12}S_4$ $[M + H]^+$: 1158.1453; found: 1158.1429 (Supporting Information Figures S2 and S3).

To a solution of DA-modified cnxtls (1 mg in 150 μL MeOH, 0.1 μmol of reactive aldehyde) was added **1** (72 μg, in 200 μL MeOH,) and glacial acetic acid (20 μL) at ambient temperature (Scheme 2). The resulting reaction mixture was heated to 40 °C and agitated by the thermomixer in the dark for 3 h. Sodium cyanoborohydride (35 μL, 1 M in THF) was added and the reaction mixture was kept at 40 °C and agitated by the thermomixer in dark for another 3 days. The resulting dyed cnxtls were collected by centrifugation (14 000 rpm, 10 min), washed with MeOH (5 × 2 mL) and resuspended in deionized H_2O (0.25 mL) to give **3** as a 4 mg/mL solution. The amount of dye grafted to the DA-modified cnxtls was 6.3 μg/mg cellulose. When the amount of **1** is stoichiometric with the number of aldehyde groups, the recovered cnxtls are visibly colored. The amount of dye grafted to the cnxtls was 6.3 μg/mg cellulose, representing ca. 10% of the original dye in the reaction bound to the DA-modified cnxtls, 12% of the oxidized glucose rings modified, and 0.1% of the total glucose units modified.

As a control experiment, a solution of DA-modified cnxtls were reacted with **1** under the same reaction conditions except that sodium cyanoborohydride was not added. The resulting DA-modified cnxtls did not retain color through the washing procedure, yielding a white product.

Conjugation of Alexa Fluor 546 to Cellulose Nanocrystals with a Triazine Linkage. Compound **1** was prepared as previously mentioned except starting with 100 μg (in 100 μL MeOH, 0.0967 μmol) Alexa Fluor 546 C_5 maleimide. To a stirred and cooled (0 °C) solution of cyanuric chloride (0.46 mg, 2.5 μmol) and Na_2CO_3 (2 mg) in anhydrous CH_3CN (0.2 mL) under an atmosphere of N_2 was added **1** (in 0.3 mL MeOH) dropwise (Scheme 1). The reaction mixture was stirred for 3 h at the same temperature. The reaction progress was analyzed by ESI-QTof MS. Unreacted cyanuric chloride was removed by preparative TLC (EtOAc/hexanes, 1/1, v/v) and after evaporation of solvent by a stream of N_2, to give **2** (100 μg, 87%) as a purple solid. High resolution ESI-QTof MS of **2**: *m/z* calcd for $C_{53}H_{53}Cl_4N_8NaO_{13}S_4$ $[M + H]^+$: 1301.1339; found: 1301.1223 (Supporting Information Figures S4 and S5).

A suspension of cellulose nanocrystals in dry acetonitrile was prepared from aqueous suspension by centrifugation and repeated washing with anhydrous acetonitrile. A solution of cnxtls (2 mg in 600 μL CH_3CN, 0.012 mmol) was added to **2** (100 μg) and Na_2CO_3 (4 mg) at ambient temperature (Scheme 3, compound **2** is sparingly soluble in CH_3CN at room temperature). The resulting reaction mixture was heated to 65 °C and agitated by the thermomixer in dark for 36 h. The resulting dyed cnxtls were collected by centrifugation (14 000 rpm, 10 min), washed and sonicated successively with MeOH (5 × 2 mL), DMF (5 × 2 mL), DMSO (5 × 2 mL), and deionized H_2O (5 × 2 mL) to remove all unreacted dye; the resulting cnxtls are visibly colored. The resulting cnxtls were resuspended in deionized H_2O (0.5 mL) to give **4** as a 4 mg/mL solution. The amount of dye grafted to the cellulose nanocrystals was 3.3 μg/mg cellulose, representing ca. 8% of the original dye in the reaction bound to the cnxtls, and 0.05% of the total glucose units modified.

Degree of Labeling. The degree of labeling of Alexa Fluor dyes on cellulose nanocrystals materials **3** and **4** were determined from their UV−vis absorbance spectra. As shown in figures in the SI, the absorbance intensity of cellulose nanocrystals **3** and **4** at 556 nm were found to be 0.87 and 0.46, respectively. The amount of dye attached on each cellulose nanocrystals was calculated by correlating the absorbance intensity against a calibration curve obtained from known concentration of free dyes in water.

Micromodel Fabrication. To create micromodels, SU-8 50 (Microchem, Newton, MA) was spin-coated on a 100 mm Si wafer at 1250 rpm for 30 s after which the wafer was soft-baked on hot plates at 65 and 95 °C for 10 and 30 min, respectively. The wafer was then exposed to UV radiation through a chromium-on-glass photomask that was patterned in-house using a SF-100 maskless lithography system (Intelligent Micropatterning, St. Petersburg, FL). Exposure took place in a Neutronix-Quintel 4006 photomask aligner (Morgan Hill, CA). Following exposure, the wafer was postexposure baked at 65 and 95 °C for 2 and 8 min, respectively, and then developed in SU-8 developer (Microchem). The patterned wafer was then hard-baked at 180 °C for 30 min to complete template fabrication.

PDMS base and curing agent (Dow Corning Sylgard 184, Ellsworth Adhesives, Germantown, WI) were thoroughly mixed and then poured over the template to a thickness of ∼3 mm. The poured PDMS was degassed under vacuum for 30 min and

DOI: 10.1021/acs.bioconjchem.5b00048
Bioconjugate Chem. 2015, 26, 593−601

then cured in an oven at 75 °C for 2 h. After curing, the patterned micromodels were excised from the mold with a razor blade. Fluid access holes were formed using a punch. Images of a full PDMS micromodel and the apparatus designed to clamp it to a glass substrate are shown in Supporting Information Figure S14.

■ ASSOCIATED CONTENT

Supporting Information

Figures S1−S15 provide additional experimental results. This material is available free of charge via the Internet at http://pubs.acs.org/.

■ AUTHOR INFORMATION

Corresponding Author

*E-mail: jwgrate@pnnl.gov. Fax: 509-371-6242. Tel: 509-371-6500.

Present Addresses

Andreas Vasdekis, Department of Physics, University of Idaho, Moscow, ID, 83844

Michael J. Wilkins, School of Earth Sciences and Department of Microbiology, The Ohio State University, Columbus, OH, 43210

Notes

The authors declare no competing financial interest.

■ ACKNOWLEDGMENTS

The authors would like to acknowledge Jonathan W. Pittman for his efforts early in this project. Shicheng Chen, Michigan State University, is thanked for providing the Flavobacterium strain used in this study. This research was supported as part of the Microbial Communities Initiative by the Laboratory Directed Research and Development Program at Pacific Northwest National Laboratory (PNNL), a multiprogram national laboratory operated by Battelle for the U.S. Department of Energy (DOE). A portion of this research was carried out in the William R. Wiley Environmental Molecular Sciences Laboratory (EMSL), a DOE Office of Science User Facility sponsored by the Office of Biological and Environmental Research and located at PNNL.

■ REFERENCES

(1) Morandi, G., and Thielemans, W. (2012) Synthesis of cellulose nanocrystals bearing photocleavable grafts by ATRP. *Polym. Chem. 3*, 1402−1407.

(2) Dong, S., and Roman, M. (2007) Fluorescently labeled cellulose nanocrystals for bioimaging applications. *J. Am. Chem. Soc. 129*, 13810−13811.

(3) Eyley, S., Shariki, S., Dale, S. E. C., Bending, S., Marken, F., and Thielemans, W. (2012) Ferrocene-decorated nanocrystalline cellulose with charge carrier mobility. *Langmuir 28*, 6514−6519.

(4) Hassan, M. L., Moorefield, C. M., Elbatal, H. S., Newkome, G. R., Modarelli, D. A., and Romano, N. C. (2012) Fluorescent cellulose nanocrystals via supramolecular assembly of terpyridine-modified cellulose nanocrystals and terpyridine-modified perylene. *Mater. Sci. Eng., B 177*, 350−358.

(5) Filpponen, I., Sadeghifar, H., and Argyropoulos, D. S. (2011) Photoresponsive cellulose nanocrystals. *Nanomater. Nanotechnol. 1*, 34−43.

(6) Majoinen, J., Walther, A., McKee, J. R., Kontturi, E., Aseyev, V., Malho, J. M., Ruokolainen, J., and Ikkala, O. (2011) Polyelectrolyte brushes grafted from cellulose nanocrystals using Cu-mediated surface-initiated controlled radical polymerization. *Biomacromolecules 12*, 2997−3006.

(7) Sadeghifar, H., Filpponen, I., Clarke, S. P., Brougham, D. F., and Argyropoulos, D. S. (2011) Production of cellulose nanocrystals using hydrobromic acid and click reactions on their surface. *J. Mater. Sci. 46*, 7344−7355.

(8) Nielsen, L. J., Eyley, S., Thielemans, W., and Aylott, J. W. (2010) Dual fluorescent labelling of cellulose nanocrystals for pH sensing. *Chem. Commun. 46*, 8929−8931.

(9) Abeer, M. M., Mohd. Amin, M. C. I., and Martin, C. (2014) A review of bacterial cellulose-based drug delivery systems: their biochemistry, current approaches and future prospects. *J. Pharm. Pharmacol. 66*, 1047−1061.

(10) Czaja, W. K., Young, D. J., Kawecki, M., and Brown, R. M. (2006) The future prospects of microbial cellulose in biomedical applications. *Biomacromolecules 8*, 1−12.

(11) Xu, F. J., Zhu, Y., Liu, F. S., Nie, J., Ma, J., and Yang, W. T. (2010) Comb-shaped conjugates comprising hydroxypropyl cellulose backbones and low-molecular-weight poly(N-isopropylacryamide) side chains for smart hydrogels: synthesis, characterization, and biomedical applications. *Bioconjugate Chem. 21*, 456−464.

(12) Song, Y., Wang, H., Zeng, X., Sun, Y., Zhang, X., Zhou, J., and Zhang, L. (2010) Effect of molecular weight and degree of substitution of quaternized cellulose on the efficiency of gene transfection. *Bioconjugate Chem. 21*, 1271−1279.

(13) Edwards, J. V., Sethumadhavan, K., and Ullah, A. H. J. (2000) Conjugation and modeled structure/function analysis of lysozyme on glycine esterified cotton cellulose-fibers. *Bioconjugate Chem. 11*, 469−473.

(14) Schimel, D., Alves, D., Enting, I., Heimann, M., Joos, F., Raynaud, D., and Wigley, T. (1996) CO_2 and the carbon cycle, in *Climate Change 1995: The Science of Climate Change. Contribution of Working Group I to the Second Assessment Report of the IPCC* (Houghton, J. T., et al., Ed.) pp 65−86, Cambridge University Press, Cambridge.

(15) Vargas, R., Carbone, M. S., Reichstein, M., and Baldocchi, D. D. (2011) Frontiers and challenges in soil respiration research: from measurements to model-data integration. *Biogeochemistry 102*, 1−13.

(16) Heimann, M., and Reichstein, M. (2008) Terrestrial ecosystem carbon dynamics and climate feedbacks. *Nature 451*, 289−292.

(17) Reichstein, M., and Beer, C. (2008) Soil respiration across scales: The importance of a model−data integration framework for data interpretation. *J. Plant Nutr. Soil Sci. 171*, 344−354.

(18) Sharrock, K. R. (1988) Cellulase assay methods: a review. *J. Biochem. Biophys. Methods 17*, 81−105.

(19) Helbert, W., Chanzy, H., Husum, T. L., Schulein, M., and Ernst, S. (2003) Fluorescent cellulose microfibrils as substrate for the detection of cellulase activity. *Biomacromolecules 4*, 481−487.

(20) Bondeson, D., Mathew, A., and Oksman, K. (2006) Optimization of the isolation of nanocrystals from microcrystalline cellulose by acid hydrolysis. *Cellulose 13*, 171−180.

(21) Filpponen, I. (2009) in *Department of Wood and Paper Science* pp 202, North Carolina State University.

(22) Habibi, Y., Lucia, L. A., and Rojas, O. J. (2010) Cellulose nanocrystals: chemistry, self-assembly, and applications. *Chem. Rev. 110*, 3479−3500.

(23) Klemm, D., Kramer, F., Moritz, S., Lindstroem, T., Ankerfors, M., Gray, D., and Dorris, A. (2011) Nanocelluloses: a new family of nature-based materials. *Angew. Chem., Int. Ed. 50*, 5438−5466.

(24) Kontturi, E., Johansson, L.-S., Kontturi, K. S., Ahonen, P., Thuene, P. C., and Laine, J. (2007) Cellulose nanocrystal submonolayers by spin coating. *Langmuir 23*, 9674−9680.

(25) Moon, R. J., Martini, A., Nairn, J., Simonsen, J., and Youngblood, J. (2011) Cellulose nanomaterials review: structure, properties and nanocomposites. *Chem. Soc. Rev. 40*, 3941−3994.

(26) Siqueira, G., Bras, J., and Dufresne, A. (2010) Cellulosic bionanocomposites: A review of preparation, properties and applications. *Polymers (Basel, Switz.) 2*, 728−765.

(27) Eyley, S., and Thielemans, W. (2011) Imidazolium grafted cellulose nanocrystals for ion exchange applications. *Chem. Commun. 47*, 4177−4179.

DOI: 10.1021/acs.bioconjchem.5b00048
Bioconjugate Chem. 2015, 26, 593−601

(28) Alissandratos, A., Baudendistel, N., Hauer, B., Baldenius, K., Flitsch, S., and Halling, P. (2011) Biocompatible functionalisation of starch. *Chem. Commun. 47*, 683−685.
(29) Panchuk-Voloshina, N., Haugland, R., Bishop-Stewart, J., Bhalgat, M. K., Millard, P. J., Mao, F., Leung, W.-Y., and Haugland, R. P. (1999) Alexa dyes, a series of new fluorescent dyes that yield exceptionally bright, photostable conjugates. *J. Histochem. Cytochem. 47*, 1179−1188.
(30) Kim, U.-J., Kuga, S., Wada, M., Okano, T., and Kondo, T. (2000) Periodate oxidation of crystalline cellulose. *Biomacromolecules 1*, 488−492.
(31) Kim, U.-J., Wada, M., and Kuga, S. (2004) Solubilization of dialdehyde cellulose by hot water. *Carbohydr. Polym. 56*, 7−10.
(32) Lindh, J., Carlsson, D. O., Strømme, M., and Mihranyan, A. (2014) Convenient one-pot formation of 2,3-dialdehyde cellulose beads via periodate oxidation of cellulose in water. *Biomacromolecules 15*, 1928−1932.
(33) Jackson, E. L., and Hudson, C. S. (1937) Studies on the cleavage of the carbon chain of glycosides by oxidation. A new method for determining ring structures and alpha and beta configurations of glycosides1. *J. Am. Chem. Soc. 59*, 994−1003.
(34) Bruneel, D., and Schacht, E. (1993) Chemical modification of pullulan: 1. Periodate oxidation. *Polymer 34*, 2628−2632.
(35) Blotny, G. (2006) Recent applications of 2,4,6-trichloro-1,3,5-triazine and its derivatives in organic synthesis. *Tetrahedron 62*, 9507−9522.
(36) Dawson, T. L., Fern, A. S., and Preston, C. (1960) The reactions of cold-dyeing procion dyes with cellulose. *Journal of the Society of Dyers and Colourists 76*, 210−217.
(37) Rattee, I. D. (1969) Reactive dyes in the coloration of cellulosic materials. *Journal of the Society of Dyers and Colourists 85*, 23−31.
(38) Liang, K., and Chen, Y. (2012) Elegant chemistry to directly anchor intact saccharides on solid surfaces used for the fabrication of bioactivity-conserved saccharide microarrays. *Bioconjugate Chem. 23*, 1300−1308 DOI: 10.1021/bc300142s.
(39) Lenormand, R. (1999) Visualization of flow patterns in 2D model networks, in *Experimental Methods in the Physical Sciences* (Celotta, R., and Lucatorto, T., Eds.) pp 43−67, Academic Press, San Diego.
(40) Willingham, T. W., Werth, C. J., and Valocchi, A. J. (2008) Evaluation of the effects of porous media structure on mixing-controlled reactions using pore-scale modeling and micromodel experiments. *Environ. Sci. Technol. 42*, 3185−3193.
(41) Berejnov, V., Djilali, N., and Sinton, D. (2008) Lab-on-chip methodologies for the study of transport in porous media: energy applications. *Lab Chip 8*, 689−693.
(42) Grate, J. W., Zhang, C. Y., Wietsma, T. W., Warner, M. G., Anheier, N. C., Bernacki, B. E., Orr, G., and Oostrom, M. (2011) A note on the visualization of wetting film structures and a nonwetting immiscible fluid in a pore network micromodel using a solvatochromic dye. *Water Resour. Res. 46*, W11602.
(43) Wu, M., Xiao, F., Johnson-Paben, R. M., Retterer, S. T., Yin, X., Neeves, K. B. (2012) Single- and two-phase flow in microfluidic porous media analogs based on Voronoi tessellation. *Lab Chip 12*.
(44) Zhang, C. Y., Oostrom, M., Wietsma, T. W., Grate, J. W., and Warner, M. G. (2011) Influence of viscous and capillary forces on immiscible fluid displacement: pore-scale experimental study in a water-wet micromodel demonstrating viscous and capillary fingering. *Energy Fuels 25*, 3493−3505.
(45) Zhang, C. Y., Kang, Q. J., Wang, X., Zilles, J. L., Muller, R. H., and Werth, C. J. (2010) Effects of pore-scale heterogeneity and transverse mixing on bacterial growth in porous media. *Environ. Sci. Technol. 44*, 3085−3092.
(46) Grate, J. W., Dehoff, K. J., Warner, M. G., Pittman, J. W., Wietsma, T. W., Zhang, C. Y., and Oostrom, M. (2012) Correlation of oil-water and air-water contact angles of diverse silanized surfaces and relationship to fluid interfacial tensions. *Langmuir 28*, 7182−7188.

DOI: 10.1021/acs.bioconjchem.5b00048
Bioconjugate Chem. 2015, 26, 593−601